

Tourmaline crystal chemistry

FERDINANDO BOSI^{1,*}

¹Department of Earth Sciences, Sapienza University di Rome, Piazzale Aldo Moro 5, 00185 Rome, Italy

ABSTRACT

Tourmalines form the most important boron rock-forming minerals on Earth. They belong to the cyclosilicates with a structure that may be regarded as a three-dimensional framework of octahedra ZO_6 that encompass columns of structural “islands” made of XO_9 , YO_6 , BO_3 , and TO_4 polyhedra. The overall structure of tourmaline is a result of short-range and long-range constraints resulting, respectively on the charge and size of ions. In this study, published data are reviewed and analyzed to achieve a synthesis of relevant experimental results and to construct a crystal-chemical model for describing tourmalines and their compositional miscibility over different length scales. Order-disorder substitution reactions involving cations and anions are controlled by short-range structural constraints, whereas order-disorder intracrystalline reaction involving only cations are controlled by long-range structural constraints. The chemical affinity of a certain cation to a specific structural site of the tourmaline structure has been established on the basis of structural data and crystal-chemical considerations. This has direct implications for the tourmaline nomenclature, as well as on petrogenetic and provenance information. Some assumptions behind the classification scheme of tourmaline have been reformulated, revealing major agreement and significant improvements compared to earlier proposed scheme.

Keywords: Tourmaline, order-disorder, crystal structure, nomenclature

INTRODUCTION

The tourmaline supergroup minerals are chemically complex cyclosilicates rich in boron. They are the most common and the earliest boron minerals formed on Earth (Grew et al. 2016). Tourmalines are widespread in Earth’s crust, typically occurring in granites and granitic pegmatites but also in sedimentary and metamorphic rocks (Dutrow and Henry 2011; van Hinsberg et al. 2011). Tourmalines also preserve important records of the geological conditions in which they form in the lithosphere, thus it is important that we understand how to read these records (e.g., Dutrow and Henry 2011). The general formula may be written as: $XY_3Z_6T_6O_{18}(BO_3)_3V_3W$, with $X = Na^+, K^+, Ca^{2+}, \square$ (= vacancy); $Y = Al^{3+}, Cr^{3+}, V^{3+}, Fe^{2+/3+}, Mg^{2+}, Mn^{2+}, Li^+, Ti^{4+}$; $Z = Al^{3+}, Cr^{3+}, V^{3+}, Fe^{2+/3+}, Mg^{2+}$; $T = Si^{4+}, Al^{3+}, B^{3+}$; $B = B^{3+}$, $V = (OH)^-, O^{2-}$; $W = (OH)^-, F^-, O^{2-}$ being the most common constituents. The letters in the formula (X, Y, Z, T , and B , not italicized) represent groups of cations at the ^[9] X , ^[6] Y , ^[6] Z , ^[4] T , and ^[3] B crystallographic sites (letters italicized). The letters V and W represent groups of anions at the ^[3] $O3$ and ^[3] $O1$ sites, respectively. The H atoms occupy the $H3$ and $H1$ sites, which are related to $O3$ and $O1$, respectively.

Since the publication of the nomenclature of the tourmaline-supergroup minerals (Henry et al. 2011), several new members of tourmaline have been approved by the Commission on New Minerals, Nomenclature and Classification (CNMNC) of the International Mineralogical Association (IMA). These include oxy-species characterized by high contents of Al^{3+} , Cr^{3+} , V^{3+} , and $Fe^{2+/3+}$, which have provided a better understanding of the tourmaline crystal chemistry. This paper will present a general

picture of the tourmaline structure and crystal chemistry, showing major factors controlling stability and chemical constraints from a short- and long-range structural viewpoint. The critical recognition of the importance of charge and size of atoms in determining crystal-chemical properties and miscibility behavior will be emphasized as well as critical comments on the assumptions behind the classification scheme of tourmaline. The importance of the crystal-chemical control of the tourmaline composition has direct implications on nomenclature as well as on the petrogenetic and provenance information (e.g., Hawthorne and Henry 1999).

TOURMALINE CONSTITUENTS AND SPECIES

The compositional range of tourmaline is remarkable, including important constituents with more than one oxidation state (e.g., Fe^{2+} - Fe^{3+} and Mn^{2+} - Mn^{3+}) and other characterizing synthetic tourmalines (e.g., Ag^+ , Co^{2+} , Ni^{2+} , Cu^{2+} , and Ga^{3+} ; London et al. 2006; Rozhdestvenskaya et al. 2012; Vereshchagin et al. 2013, 2015, 2016). A total of (at least) 26 relevant constituents, in terms of concentration or occurrence, have been unambiguously identified in tourmaline (Table 1). These constituents are very different in charge and size and accommodate into 7 crystallographic sites ($X, Y, Z, T, B, O1$, and $O3$); the other sites ($O2, O4, O5, O6, O7$, and $O8$) are solely occupied by oxygen. Moreover, the number of constituent-coordination environments is relatively large, compared to most other minerals: [3], [4], [6], and [9] coordination. Thus, tourmaline violates the Pauling’s parsimony rule, which emphasizes that the number of topochemically different environments in a structure tends to be small (Hawthorne 2006). In theory, this relatively large number of substantially different sites would decrease the stability, but tourmaline exists over environments that extend from the surface of the crust to the

* E-mail: ferdinando.bosi@uniroma1.it

TABLE 1. The 26 relevant constituents occurring in tourmaline

Valence	0	1	2	3	4
	^{[9]-[6]]} □	^[9] Na ⁺	^[9] Ca ²⁺	^{[6]-[4]]} Al ³⁺	^[4] Si ⁴⁺
		^[9] K ⁺	^[6] Mg ²⁺	^[6] Cr ³⁺	^[6] Ti ⁴⁺
		^[6] Li ⁺	^[6] Fe ²⁺	^[6] V ³⁺	
		^[9] Ag ⁺	^[6] Mn ²⁺	^[6] Fe ³⁺	
		H⁺	^[6] Ni ²⁺	^[6] Ga ³⁺	
		^[3] F ⁻	^[6] Co ²⁺	^{[3]-[4]]} B ³⁺	
			^[6] Cu ²⁺	^[6] Mn ³⁺	
			^[6] Zn ²⁺		
			^{[3]-[4]]} O ²⁻		

Notes: Vacancy (□) is considered as a constituent in accord with the IMA-CNMNC rules. Brackets indicate coordination numbers. Bold indicates constituents characterizing the 33 species of the tourmaline-supergroup minerals.

upper mantle (e.g., Marschall et al. 2009; Lussier et al. 2016) in the presence of H₂O, B-, and F-bearing fluids.

The dominance of tourmaline constituents at one or more sites of the structure gives rise to a range of mineral species. At present, the tourmaline supergroup consists of 33 mineral species approved by the IMA-CNMNC (Table 2).

CRYSTAL STRUCTURE

The tourmaline structure is typically rhombohedral, space group *R3m* with *Z* = 3, although some studies report lower symmetry such as orthorhombic, monoclinic, or triclinic (e.g., Akizuki et al. 2001; Shtukenberg et al. 2007; Hughes et al. 2011). Tourmaline has an intermediate structural complexity of about 200 bits per unit cell (Krivovichev 2013), which is larger than that of amphibole (about 150 bits per unit cell), but smaller than that of some other minerals such as analcime (usually much over 200 bits per unit cell).

The tourmaline structure may be regarded as one of the most elegant of all crystal structures. It belongs to the subclass of cyclosilicate as consists of rings of six *TO*₄ tetrahedra, lying in a plane parallel to (0001). Because all tetrahedra point in the same direction, tourmaline lacks center symmetry (polar character) and is both pyroelectric and piezoelectric (electrical properties). Each tetrahedron shares one edge with the trigonal antiprism *XO*₉, which is located along the threefold axis passing through the center of each six-membered ring [*T*₆*O*₁₈]. The *X*-site occupancy usually reflects the paragenesis of the rock in which tourmaline crystallizes (petrologic information), and tourmaline supergroup is classified into primary groups based on the dominant occupancy of the *X* site: vacant, alkali, and calcic groups (Henry et al. 2011). The antiprism *XO*₉ and the ring [*T*₆*O*₁₈] combine with two sets of three octahedra *YO*₆: an [*Y*₃*O*₁₅] triplet of octahedra caps the *XO*₉ polyhedron toward the +*c* axis and the other [*Y*₃*O*₁₃] caps the [*T*₆*O*₁₈] ring of tetrahedra toward the -*c* axis. The most extensive compositional variation occurs at the *Y* site, which is able to incorporate constituents of different sizes and charges (including vacancies) that makes tourmaline famous for its extensive range of colors (all rainbow colors) even within individual crystals (oscillatory and sector zoning). The *BO*₃ groups oriented sub-parallel to (0001) lie between the tetrahedral rings and are fully occupied by B, which makes tourmaline one of the most important B-bearing minerals (reservoir of B) in the Earth. The structural arrangement of [*T*₆*O*₁₈], *XO*₉, [*Y*₆*O*₁₈], and (*BO*₃)₃ form “islands” that are stacked in columns along the *c* axis. These islands are attached to one another along the *a* and *b* crystallographic axes by spiral chains of *ZO*₆ octahedra (Fig. 1),

TABLE 2. The 33 mineral species of tourmaline recognized by the IMA-CNMNC

Adachiite	CaFe ³⁺ Al ₆ (Si ₅ AlO ₁₈)(BO ₃) ₃ (OH) ₃ OH
Bosiite	NaFe ³⁺ (Al ₁ Mg ₂)Si ₆ O ₁₈ (BO ₃) ₃ (OH) ₃ O
Chromium-dravite	NaMg ₃ Cr ₆ Si ₆ O ₁₈ (BO ₃) ₃ (OH) ₃ OH
Chromo-alumino-povondraite	NaCr ₃ (Al ₄ Mg ₂)Si ₆ O ₁₈ (BO ₃) ₃ (OH) ₃ O
Darrellhenryite	NaLiAl ₂ Al ₆ Si ₆ O ₁₈ (BO ₃) ₃ (OH) ₃ O
Dravite	NaMg ₃ Al ₆ Si ₆ O ₁₈ (BO ₃) ₃ (OH) ₃ OH
Elbaite	Na(Li _{1.5} Al _{1.5})Al ₆ Si ₆ O ₁₈ (BO ₃) ₃ (OH) ₃ OH
Feruvite	CaFe ³⁺ (MgAl ₂)Si ₆ O ₁₈ (BO ₃) ₃ (OH) ₃ OH
Fluor-buergerite	NaFe ³⁺ Al ₆ Si ₆ O ₁₈ (BO ₃) ₃ O ₃ F
Fluor-dravite	NaMg ₃ Al ₆ Si ₆ O ₁₈ (BO ₃) ₃ (OH) ₃ F
Fluor-elbaite	Na(Li _{1.5} Al _{1.5})Al ₆ Si ₆ O ₁₈ (BO ₃) ₃ (OH) ₃ F
Fluor-liddicoatite	Ca(Li ₂ Al)Al ₆ Si ₆ O ₁₈ (BO ₃) ₃ (OH) ₃ F
Fluor-schorl	NaFe ³⁺ Al ₆ Si ₆ O ₁₈ (BO ₃) ₃ (OH) ₃ F
Fluor-tsilaite	NaMn ³⁺ Al ₆ Si ₆ O ₁₈ (BO ₃) ₃ (OH) ₃ F
Fluor-uvite	CaMg ₃ (Al ₃ Mg)Si ₆ O ₁₈ (BO ₃) ₃ (OH) ₃ F
Foitite	□(Fe ²⁺ Al)Al ₆ Si ₆ O ₁₈ (BO ₃) ₃ (OH) ₃ OH
Lucchesiite	CaFe ³⁺ Al ₆ Si ₆ O ₁₈ (BO ₃) ₃ (OH) ₃ O
Luinaite-(OH) ^a	(Na,□)(Fe ²⁺ ,Mg) ₃ Al ₆ Si ₆ O ₁₈ (BO ₃) ₃ (OH) ₃ OH
Magnesian-foitite	□(Mg ₂ Al)Al ₆ Si ₆ O ₁₈ (BO ₃) ₃ (OH) ₃ OH
Maruyamaite	K(Al ₂ Mg)(Al ₄ Mg)Si ₆ O ₁₈ (BO ₃) ₃ (OH) ₃ O
Olenite	NaAl ₃ Al ₃ Si ₆ O ₁₈ (BO ₃) ₃ O ₃ OH
Oxy-chromium-dravite	NaCr ₃ (Cr ₄ Mg ₂)Si ₆ O ₁₈ (BO ₃) ₃ (OH) ₃ O
Oxy-dravite	Na(Al ₂ Mg)(Al ₂ Mg)Si ₆ O ₁₈ (BO ₃) ₃ (OH) ₃ O
Oxy-foitite	□(Al ₂ Fe ²⁺)Al ₆ Si ₆ O ₁₈ (BO ₃) ₃ (OH) ₃ O
Oxy-schorl	Na(Fe ²⁺ Al)Al ₆ Si ₆ O ₁₈ (BO ₃) ₃ (OH) ₃ O
Oxy-vanadium-dravite	NaV ₃ (V ₄ Mg ₂)Si ₆ O ₁₈ (BO ₃) ₃ (OH) ₃ O
Povondraite	NaFe ³⁺ (Fe ³⁺ ,Mg ₂)Si ₆ O ₁₈ (BO ₃) ₃ (OH) ₃ O
Rossmannite	□(Al ₂ Li)Al ₆ Si ₆ O ₁₈ (BO ₃) ₃ (OH) ₃ OH
Schorl	NaFe ³⁺ Al ₆ Si ₆ O ₁₈ (BO ₃) ₃ (OH) ₃ OH
Tsilaite	NaMn ³⁺ Al ₆ Si ₆ O ₁₈ (BO ₃) ₃ (OH) ₃ OH
Uvite	CaMg ₃ (Al ₃ Mg)Si ₆ O ₁₈ (BO ₃) ₃ (OH) ₃ OH
Vanadio-oxy-chromium-dravite	NaV ₃ (Cr ₄ Mg ₂)Si ₆ O ₁₈ (BO ₃) ₃ (OH) ₃ O
Vanadio-oxy-dravite	NaV ₃ (Al ₄ Mg ₂)Si ₆ O ₁₈ (BO ₃) ₃ (OH) ₃ O

^a Mineral (IMA 2009-046) description has not yet been published in the scientific literature.

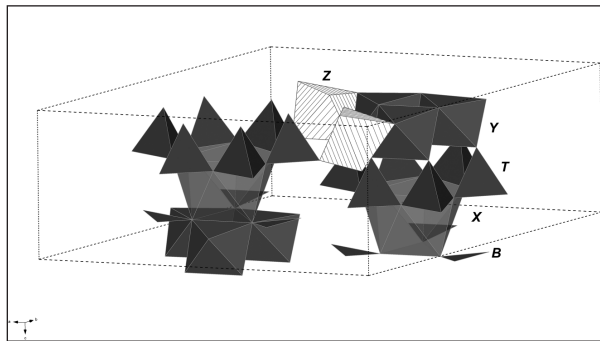


FIGURE 1. Polyhedral arrangements in the tourmaline crystal structure. Dark-gray polyhedra coordinate the *Y*, *T*, *X*, and *B* sites. Stripe-filled octahedra coordinate the *Z* site. Dashed-line represents the unit cell.

which also extend along to the *c* axis according to a 3₁ triad screw axis. The three-dimensional framework of the tourmaline structure is therefore given by the screw-like arrangement of *ZO*₆ (Fig. 2). This framework is characterized by similar strong *Z*-*O* bonds (~0.5 valence units), which would explain some physical properties: hardness (~7–7½ Mohs), lack of cleavage, resistance to weathering in clastic sediments (like rutile and zircon), and extensive pressure-temperature stability up to about 7 GPa and 950 °C. Finally, another important feature of the tourmaline structure is provided by the orientation of the hydrogen atoms, which are sub-parallel to the *c* axis: H1-hydrogen point down -*c* toward the oxygen at O1, and H3-hydrogen points up +*c* toward

the oxygen at O3. Owing to this orientation of (OH) dipoles, the fundamental (OH)-stretching bands in infrared spectra of tourmalines will display a very strong pleochroism, with $\epsilon \gg \omega$ (e.g., Skogby et al. 2012). All polyhedra discussed above are distorted. With respect to the ideal volume, bond distance or bond angle, the distortion of polyhedra decrease with decreasing coordination number according to the sequence: $XO_6 > YO_6 > ZO_6 > TO_4 > BO_3$ (Ertl et al. 2002; Bosi and Lucchesi 2007).

In summary, the tourmaline structure may be considered as a three-dimensional framework of octahedra ZO_6 that must be able to accommodate the structural islands.

STRUCTURAL CONSTRAINTS

Henry and Dutrow (2011) showed that the accommodation of F at the O1 site is influenced by the cation occupancy (total charge) of the *X* and the *Y* sites. They suggested that the manner in which chemical constituents are incorporated into the tourmaline structure depends on external influences (temperature, pressure, mineral local assemblages, and fluid composition) and on internal influences (crystallographic constraints). Moreover, tourmaline may be extremely optically, chemically, and isotopically zoned due to the occurrence of extensive short-range order of atoms that may strongly decrease the diffusion rates of atoms in the structure (e.g., Hawthorne and Dirlam 2011).

In general, the tourmaline chemical composition and zoning is a result of external and internal constraints. The latter act from a scale of a few angstroms (short-range structure) to a scale that involve the complete crystal (long-range structure).

Short-range structure

Short-range structure involves a set of atoms (cluster) that do not obey to the translational symmetry. Each cluster is controlled by bond-valence requirements, i.e., the charge of ions needs to be neutralized locally by nearest neighbors. Of particular relevance for tourmaline are the local atomic arrangements around the O1 (bonded to 3*Y*) and O3 (bonded to *Y*+2*Z*) sites, which show a greater chemical variability. Hawthorne (1996, 2002) and Bosi (2010, 2011, 2013) evaluated possible atomic arrangements

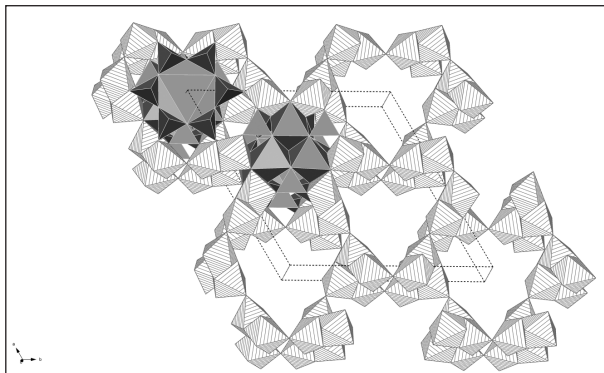


FIGURE 2. The crystal structure of a rhombohedral *R3m* tourmaline projected onto (001). Dark-gray polyhedra represent structural islands. Stripe-filled octahedra coordinate the *Z* site. Dashed-line represents the unit cell.

around O1 and O3, constrained by the valence-sum rule. According to the Bond Valence Model (e.g., Brown 2016), there is a tendency for the sum of the bond valences (BVS) around each atom to approach its formal valence (FV); if a large mismatch between BVS and FV occur, it is indicative of strained bonds that lead to instability in the structure. As a result, those local arrangements that most closely conform to the valence-sum rule are the arrangements that are most likely to occur in the structure (Hawthorne et al. 2005; Hawthorne 2016). The allowed stable short-range arrangements expressed as charge arrangements around O1 and O3 of tourmaline are summarized in Table 3. These arrangements can be considered as short-range constraints and have significant effects on the chemistry of short-range structure. For example, in oxy-foitite, ideally $\square^Y(Fe^{2+}Al_2)^Z(Al_6)(Si_6O_{18})(BO_3)_3^{O3}(OH)_3^{O1}(O)$, the *Y* and O1 sites composition would require the short-range arrangement $^Y(Fe^{2+}+2Al)^{-O1}(O^{2-})$ rather than the chemically equivalent proportion of 33% $^Y(3Fe^{2+})^{-O1}(O^{2-}) + 67\% ^Y(3Al)^{-O1}(O^{2-})$, because the arrangement $^Y(3Fe^{2+})^{-O1}(O^{2-})$ is unstable from a bond valence perspective. Similarly, the *Y*, *Z*, and O3 sites composition requires specific proportions of short-range arrangements, 33% $[^YFe^{2+}+^Z(2Al)]^{-O3}(OH) + 67\% [^YAl+^Z(2Al)]^{-O3}(OH)$.

Therefore, the short-range constraints will tend to favor specific cation arrangements around the anions at the O1 and O3 sites. We can also note that the local arrangements around O^{2-} of Table 3 can be associated with occupants having a total charge higher than that of occupants around (OH,F). This is consistent with the study of Bosi (2013), who examined the bond valences of a large number of refined tourmaline structures and showed a well-developed linear correlation between BVS at the O1 site and MFV (mean formal valence = total charge divided by the site multiplicity) at the *Y* site: $BVS(O1) = 0.99 \times MFV(Y) - 1.20$ (see also Fig. 1 of Bosi 2013). Such a correlation indicates that

TABLE 3. Stable local charge arrangements around the O1 and O3 sites of tourmaline derived from Hawthorne (1996, 2002) and Bosi (2010, 2011, 2013)

Composition	Formal valence	Charge arrangement	MFV ^a
O1	O1 ^b	YYY	<Y>
(OH) or F	-1	(R ³⁺ + 2R ²⁺)	+1.67
(OH) or F	-1	(R ³⁺ + R ²⁺ + □)	+1.67
(OH) or F	-1	(R ³⁺ + R ²⁺ + R ⁺)	+2.00
(OH) or F	-1	(R ³⁺ + R ²⁺ + □)	+2.00
(OH) or F	-1	(3R ²⁺)	+2.00
(OH) or F	-1	(2R ²⁺ + R ⁺)	+2.33
(OH) or F	-1	(2R ²⁺ + R ³⁺)	+2.33
O	-2	(R ²⁺ + 2R ³⁺)	+2.67
O	-2	(3R ³⁺)	+3.00
O3	O3 ^b	YZZ	<YZZ>
(OH)	-1	^Y R ⁺ + ^Z (R ²⁺ + R ³⁺)	+2.00
(OH)	-1	^Y □ + ^Z (2R ³⁺)	+2.00
(OH)	-1	^Y R ⁺ + ^Z (2R ³⁺)	+2.33
(OH)	-1	^Y R ²⁺ + ^Z (R ²⁺ + R ³⁺)	+2.33
(OH)	-1	^Y R ³⁺ + ^Z (2R ²⁺)	+2.33
(OH)	-1	^Y R ²⁺ + ^Z (2R ³⁺)	+2.67
(OH)	-1	^Y R ³⁺ + ^Z (R ²⁺ + R ³⁺)	+2.67
(OH)	-1	^Y R ³⁺ + ^Z (2R ³⁺)	+3.00
O	-2	^Y R ³⁺ + ^Z (2R ³⁺)	+3.00

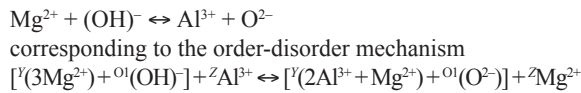
Notes: Abbreviation: R⁺, R²⁺, and R³⁺ = generalized monovalent (+1), divalent (+2), and trivalent (+3) cation.

^a MFV = mean formal valence = Total charge/3.

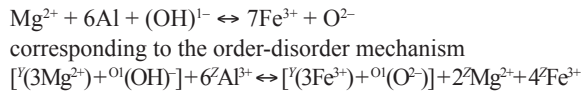
^b Because of the hydrogen bond, the bond-valence sum at the O1 and O3 sites occupied by (OH) are 1.05 and 1.15 v.u., respectively (e.g., Hawthorne 2002; Gatta et al. 2014).

${}^{01}\text{O}^{2-}$ content increases with increasing of ${}^Y\text{R}^{3+}$ content as suggested by Table 3, and may hence be considered as the linking between what predicted by bond valence arguments in the short-range structure with what observed by the diffraction techniques in the long-range structure.

As the sum of all different stable short-range arrangements corresponds to occupancies of the sites averaged over the complete crystal, it is apparent that (1) the stable short-range structures affects the long-range structure, (2) the short-range constraints may have significant effects on the variation in chemical composition of tourmalines such as atomic substitutions and order-disorder mechanisms. In this regard, consider that the relation between dravite and oxy-dravite can be formulated by the chemical substitution:

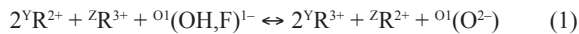


This mechanism involves the stable short-range arrangements $[{}^Y(3\text{R}^{2+}) - {}^{01}(\text{OH})]$ and $[{}^Y(2\text{R}^{3+} + \text{R}^{2+}) - {}^{01}(\text{O})]$ compatible, respectively, with dravite and oxy-dravite (or maruyamaite), and it can be simplified to $2{}^Y\text{Mg}^{2+} + {}^{01}(\text{OH})^- + {}^Z\text{Al}^{3+} \leftrightarrow 2{}^Y\text{Al}^{3+} + {}^{01}(\text{O}^{2-}) + {}^Z\text{Mg}^{2+}$ (Hawthorne 1996). Similarly, dravite and povondraite are related by the chemical substitution:



This mechanism involves the stable short-range arrangements $[{}^Y(3\text{R}^{2+}) - {}^{01}(\text{OH})]$ and $[{}^Y(3\text{R}^{3+}) - {}^{01}(\text{O})]$ compatible with dravite and povondraite, respectively.

The two mechanisms reported above can be generalized to:



which are actually order-disorder *substitution* reactions involving cations and anions and controlled by local bond-valence requirements at the O1 site, i.e., short-range constraints.

Besides order-disorder *substitution* reactions 1 and 2, there is another type of order-disorder reaction that involves only cations:



The latter is an intracrystalline reaction usually controlled by long-range constraints (see below).

Long-range structure

The short-range constraints control which atoms can be nearest neighbors and hence determine the short-range structure. The sum of all of the short-range arrangements leads to a long-range structure. The latter is determined mainly by spatial/steric constraints (imposed by translational symmetry) that restrict the number of ways in which ions can be bonded to each other in the three-dimensional space. For a long-range structure to be formed, both short-range and long-range constraints must be satisfied.

Consequently, all involved short-range arrangements need to be consistent with geometrical requirements, that is, with specific long-range interatomic distances.

In tourmaline, the three-dimensional framework of the ZO_6 polyhedra must be able to accommodate the structural islands (Fig. 2). On the basis of 127 structure refinement (SREF) data, Bosi and Lucchesi (2007) presented a structural stability field for tourmaline as a function of $\langle Y\text{-O} \rangle$ and $\langle Z\text{-O} \rangle$, suggesting that only a limited mismatch in the dimensions between $\langle Y\text{-O} \rangle$ and $\langle Z\text{-O} \rangle$ can be tolerated by the structure. At present, additional SREF can be found in the literature (at least 195, for a total of 322 data sets), which confirm the occurrence of a dimensional difference $\Delta_{Y-Z} = \langle Y\text{-O} \rangle - \langle Z\text{-O} \rangle$ in the range between 0.00 and 0.15 Å (Fig. 3). All known tourmalines fall within the delineated field indicating the presence of a long-range structural constraint. As values outside the range 0.00–0.15 Å have never been correctly observed so far, possible anomalous data need to be carefully checked: for example, the mean bond distances of lucchesiite from Czech Republic (Bosi et al. 2017a), $\langle Y\text{-O} \rangle = 2.095$ Å and $\langle Z\text{-O} \rangle = 1.932$ Å, yielded $\Delta_{Y-Z} = 0.16$ Å (>0.15 Å).

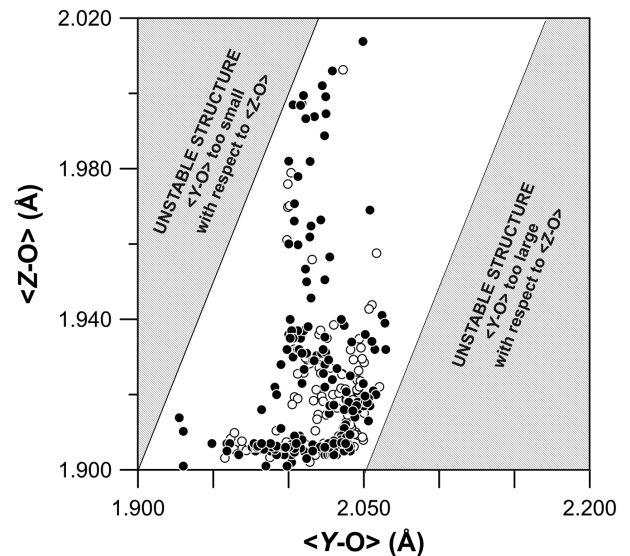


FIGURE 3. Relationship between $\langle Z\text{-O} \rangle_{\text{obs}}$ and $\langle Y\text{-O} \rangle_{\text{obs}}$ showing the possible structural-stability limits of the tourmaline supergroup. Two solid diagonal lines: left = ratio 1:1 between $\langle Z\text{-O} \rangle_{\text{obs}}$ and $\langle Y\text{-O} \rangle_{\text{obs}}$; right = ratio shifted by 0.15 Å (after Bosi and Lucchesi 2007). Plot obtained using 322 data sets with SREF: 127 (white circles) from Bosi and Lucchesi (2007, references therein) plus a total of 195 (black circles) from Razmanova et al. (1983), Marler et al. (2002; 2 sets), Ertl et al. (2006, 2007, 2008a, 2008b, 2009, 2010a, 2010b, 2010c, 2012a, 2012b, 2012c, 2013, 2015, 2016a, 2016b; 59 sets total), Kihara et al. (2007), Rozhdestvenskaya et al. (2008, 2012; 4 sets total), Bosi (2008), Lussier et al. (2008, 2011a, 2011b, 2016; 41 sets total), Bosi et al. (2010, 2012, 2013a, 2013b, 2013c, 2014a, 2014b, 2015a, 2015b, 2015c, 2016a, 2016b, 2017a, 2017b, 2017c; 40 sets total), Clark et al. (2011), Filip et al. (2012; 3 sets total), Gatta et al. (2012), Cempirek et al. (2013; 2 sets total), Bačik et al. (2013, 2015), Novák et al. (2013), Vereshchagin et al. (2013, 2014, 2015, 2016; 9 sets total), Reznitskii et al. (2014), Nishio-Hamane et al. (2014), Kutzschbach et al. (2016, 2017; 2 sets total), Berryman et al. (2016; 3 sets total), Watenphul et al. (2016), Grew et al. (2017), Bosi et al. (submitted; 7 sets total), 10 sets from Bosi (unpublished).

However, a careful check of the Y -O distances showed a mistake in the calculation of $\langle Y-O \rangle$. The correct value is actually 2.065 Å, which is fully consistent with the empirical structural constraint mentioned above: $\Delta_{Y-Z} = 0.13$ Å (< 0.15 Å).

The stability field $\langle Z-O \rangle$ vs. $\langle Y-O \rangle$ also describes and predicts the effects of the tourmaline structural stability on its chemical variability. For instance, Bosi and Lucchesi (2007) predicted that the end-member compositions of dravite, schorl, and tsilaisite (i.e., species with the Y site occupied by R^{2+} -cations and the Z site occupied by Al) should never occur, neither as natural samples nor as synthetic samples, because their structures should be unstable: $\langle {}^Y\text{Mg}-\text{O} \rangle$, $\langle {}^Y\text{Fe}^{2+}-\text{O} \rangle$, and $\langle {}^Y\text{Mn}^{2+}-\text{O} \rangle$ distances are too large with respect to $\langle {}^Z\text{Al}-\text{O} \rangle$. In this regard, the case of fluor-dravite (an oxy-free species) nicely illustrates the effect of long-range constraint on tourmaline site populations. According to the chemical analysis (Clark et al. 2011), the structural formula of fluor-dravite is expected as follows: $\text{Na}^Y(\text{Mg}_2\text{Fe}^{2+})^Z(\text{Al}_6)(\text{Si}_6\text{O}_{18})(\text{BO}_3)_3(\text{OH})_3\text{O}^{1-}[\text{F}_{0.7}(\text{OH})_{0.3}]$, with expected $\langle Y-O \rangle \sim 2.100$ Å and $\langle Z-O \rangle \sim 1.907$ Å, derived from the ionic radii (see below). These expected distances yield $\Delta_{Y-Z} = 0.19 > 0.15$ Å, indicating that the fluor-dravite structure is unstable. However, SREF data clearly show that the observed $\langle Y-O \rangle = 2.053$ Å and $\langle Z-O \rangle = 1.913$ Å are consistent with the long-range constraint ($\Delta_{Y-Z} = 0.14$ Å < 0.15 Å) because the Y and Z site population is actually disordered: $\dots^Y(\text{Mg}_{1.4}\text{Al}_{0.6}\text{Fe}_{1.0}^{2+})_{\Sigma 3.0}^Z(\text{Al}_{3.4}\text{Mg}_{0.6})_{\Sigma 6.0}\dots$ (Clark et al. 2011). In fact, the intracrystalline order-disorder reaction ${}^Y\text{Al}^{3+} + {}^Z\text{Mg}^{2+} \leftrightarrow {}^Y\text{Mg}^{2+} + {}^Z\text{Al}^{3+}$, not involving anions, occurs to shorten $\langle Y-O \rangle$ (by introducing Al^{3+}) and to enlarge $\langle Z-O \rangle$ (by introducing Mg^{2+}), thus to accommodate the potential misfit between ${}^Y\text{MgO}_6$ and ${}^Z\text{AlO}_6$.

In summary, the tourmaline structure is a result of short-range constraints depending on the charge of ions, and long-range constraints depending on the size of ions. Order-disorder substitution reactions such as 1 and 2 involve cations and anions and are controlled by the short-range constraints, whereas order-disorder (usually) intracrystalline reaction 3 involves only cations and are controlled by the long-range constraints.

THE IONIC RADII

Variations in mean bond distances are often encountered in mineral crystal structures. In accordance with the Bond Valence Model, these variations may be explained as function of the degree of strain occurring in coordination environments of cations (Bosi 2014). In line with the mineralogical convention, any variation in mean bond distance is expressed as a variation in the cation radius by keeping the anion radius fixed, although the oxide anion radius can show a wide range of values (e.g., Gibbs et al. 2014).

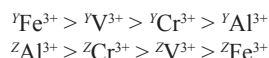
Bosi and Lucchesi (2007) refined empirical ionic radii for sixfold-coordinated ions in tourmaline and showed that the ${}^{[6]}\text{Al}$ ionic radius varies in a range of values larger than the expected one: the observed variation of $\langle {}^Z\text{Al}-\text{O} \rangle$, 1.900–1.912 Å with a grand mean value 1.906 Å (Fig. 3 of Bosi and Andreozzi 2013), is larger than 1.892 Å calculated from Shannon (1976). A significant size variation was also reported for the ${}^{[6]}\text{Fe}^{3+}$ ionic radius (0.645–0.705 Å) as well as for the other ions depending on the Y or Z site occupancy. The reasons of these variations may be ascribed to experimental errors (e.g., Bosi and Andreozzi 2013),

inductive effects from other parts of the structure (e.g., Ertl et al. 2012a), different occupancies at the octahedrally coordinated sites (e.g., Bosi and Lucchesi 2007), or more generally to different degree of strain experienced by atoms in the bonding environment (Bosi 2014).

Although the Y and Z ionic radii of Bosi and Lucchesi (2007) fitted with 93% of the Y and Z mean bond distances analyzed, their size variations are of little practical interest for crystal-chemical considerations. It is convenient to report such ionic radii by a unique mean value with its standard error ($\pm\sigma$). The latter can be estimated as the difference between the maximum and minimum radius reported in Table 2 of Bosi and Lucchesi (2007) divided by 4 or from the above mentioned distance variations for Al: $2\sigma_{\text{Al}} = \pm(1.912 - 1.900)/2 = \pm 0.006$ Å, then $\sigma_{\text{Al}} = \pm 0.003$ Å. Table 4 shows such mean ionic radii for [6]-coordinated ions in tourmaline.

CATION SITE PREFERENCE FOR Y AND Z

Because $\langle Y-O \rangle$ is always greater than $\langle Z-O \rangle$ in tourmaline, the Y site will tend to incorporate relatively large cations, whereas the Z site will tend to incorporate relatively small cations. Moreover, the chemical affinity of a certain cation to a specific structural site of the tourmaline structure can be established on the basis of structural data and crystal-chemical considerations. Bosi et al. (2017b) proposed that the preference of R^{3+} -cations for the Y and Z sites is mainly controlled by their ionic radius according to the sequence: ${}^Y\text{V}^{3+} > {}^Y\text{Cr} > {}^Y\text{Al}$ and ${}^Z\text{Al} > {}^Z\text{Cr} > {}^Z\text{V}^{3+}$. This conclusion is consistent with the cation distributions over Y and Z observed for the oxy-species such as vanadio-oxy-chromium-dravite, vanadio-oxy-dravite and chromo-alumino-povondraite (Table 2) as well as with the fact that no tourmaline species with atomic arrangements such as “... ${}^Y(\text{Al},\text{Cr})_3({}^Z\text{Mg}_2\text{V}_4)\dots$ ” have been documented so far. Ferric iron can also be included in this sequence on the basis of the Fe^{3+} -Al crystal-chemical behavior in bosiite, “... ${}^Y(\text{Fe}^{3+})_3({}^Z\text{Mg}_2\text{Al}_4)\dots$ ” (Ertl et al. 2016), and the relatively large ionic radius of Fe^{3+} . Therefore, the preference for the R^{3+} -cations to occupy the Y and Z sites is of type:



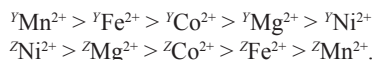
Similar arguments apply to the R^{2+} -cations (Bosi and Skogby 2013; Bosi et al. 2015a; Vereshchagin et al. 2015): the preference

TABLE 4. Empirical mean ionic radii (Å) for [6]-coordinated ions in tourmaline

Ion	This work	Shannon (1976)
Al^{3+}	0.547(3)	0.535
Cr^{3+}	0.615(1)	0.615
V^{3+}	0.655(1)	0.64
Fe^{3+}	0.675(15)	0.645
Fe^{2+}	0.776(1)	0.78
Mg^{2+}	0.722(1)	0.72
Mn^{2+}	0.809(1)	0.83
Li^+	0.751(9)	0.76

Notes: Empirical ionic radii from Shannon (1976) apply to the other ions such as $\text{Ti}^{4+} = 0.605$, $\text{Ni}^{2+} = 0.69$ Å, $\text{Co}^{2+} = 0.745$ Å, etc. The mean anionic radii $\langle \text{O} \rangle$ related to the Y and Z sites is function of constituent-anion radius of Shannon (1976). The $\langle \text{O} \rangle$ varies. From 1.35 to 1.363 Å; $\langle {}^Z\text{O} \rangle$ varies from 1.357 Å for tourmalines with $\text{O}3 = (\text{OH})$ to 1.360 Å for tourmalines with $\text{O}3 = \text{O}^{2-}$. Estimated standard error ($\pm\sigma$) in parentheses.

of R^{2+} for the Z site increases with decreasing ionic radius. An opposite preference is expected for the Y site. Therefore, the preference for the R^{2+} -cations to occupy the Y and Z sites is of type:



ON THE DEGREE OF R^{2+} - R^{3+} ORDER-DISORDER OVER THE Y AND Z SITES

In minerals, cation substitutions in a structural site are usually controlled by ion sizes (Goldschmidt's rules). In this regard, the cation-size mismatch is a useful parameter to predict the extension of chemical substitution series: size difference between ions less than $\sim 15\%$ indicates a wide substitution; by ~ 15 to $\sim 30\%$ indicates a partial substitution; more than $\sim 30\%$ indicates little substitution.

In tourmaline, the cation-size mismatch can explain the amount of R^{2+} replacing R^{3+} at the Z site, which occurs in the chemical reactions 1, 2, and 3. Using the ionic radii of Table 4, the difference in size between Al^{3+} and R^{2+} -cations are: $\text{Al-Ni}^{2+} \sim 21\%$, $\text{Al-Mg}^{2+} \sim 24\%$, $\text{Al-Co}^{2+} \sim 27\%$, $\text{Al-Fe}^{2+} \sim 30\%$, and $\text{Al-Mn}^{2+} \sim 32\%$. These values suggest the occurrence of a partial and little substitution between ${}^Z\text{Al}$ and ${}^Z\text{R}^{2+}$ -cations. The negative correlation between Al-R^{2+} cation-size mismatch and the maximum ${}^Z\text{R}^{2+}$ -occupancy observed for tourmalines with $\text{Al} > 5$ apfu, strongly supports the dependence of ionic radius on substitution degree (Fig. 4). Similarly, the different crystal-chemical behavior of ${}^Z\text{Mg}$ observed in Cr- and Al-oxy-tourmalines can be explained. As difference in size Cr^{3+} - Mg^{2+} ($\sim 15\%$) is smaller than Al-Mg^{2+} ($\sim 24\%$), the ${}^Z\text{Mg}$ content in Cr-oxy-tourmalines is expected to be larger than that in Al-oxy-tourmalines. This is confirmed by the site populations of oxy-chromium-dravite and oxy-dravite (or maruyamaite): "... ${}^Y(\text{Cr})_3$ ${}^Z(\text{Mg}_2\text{Cr}_4)$..." and "... ${}^Y(\text{MgAl}_2)$ ${}^Z(\text{MgAl}_5)$...", respectively (Bosi et al. 2012; Bosi and Skogby 2013; Lussier et al. 2016).

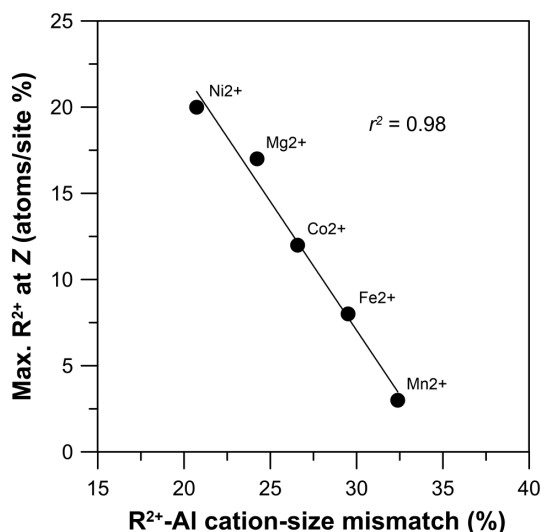


FIGURE 4. Plot of maximum occupancy of ${}^Z\text{R}^{2+}$ observed in tourmalines with $\text{Al} > 5$ apfu against R^{2+} - Al^{3+} cation-size mismatch. Solid line is linear regression. Data from Rozhdestvenskaya et al. (2012), Filip et al. (2012), Bosi and Skogby (2013), and Bosi et al. (2015b).

NOMENCLATURE ISSUES

Tourmaline site occupancies depend essentially on the charge and size of atoms forming specific arrangements that obey both the short-range and long-range structural constraints. This crystal-chemical control of tourmaline composition should be reflected in systematic procedure for classification.

The tourmaline nomenclature is based on the determination of the chemical content at each non-equivalent site of the crystal structure (Hawthorne and Henry 1999). Consequently, a structural formula $\text{XY}_3\text{Z}_6\text{T}_6\text{O}_{18}(\text{BO}_3)_3\text{V}_3\text{W}$ is required for classification purposes. In accordance with the IMA-CNMNC guidelines (e.g., Nickel and Grice 1998; Hatert and Burke 2008), this means that the chemical information of the Y and Z site should not be merged, because such sites have different crystal-chemical response to the atom accommodations. For identifying tourmaline species, Henry et al. (2011, 2013) pointed out the importance of the *empirical structural formula* stating that the "actual tourmaline structural information of the Y - and Z -site occupancy is an overriding consideration for the definition of a tourmaline species."

Only in absence of specific structural information on Y and Z occupancy, Henry et al. (2013) recommended the following site allocation procedure for the Z and Y sites: "Initially assign all Al (in excess of that assigned to the T site) to the Z site. Next, successively assign Mg^{2+} (up to 2 apfu), V^{3+} , Cr^{3+} , and Fe^{3+} . If there is an excess of trivalent cations on the Z site, the excess trivalent cations go into the Y site." As a result, tourmaline species can also be classified by combining chemical data with assumptions on the site allocation of atoms, which lead to a *calculated structural formula*. However, the application of such nomenclature rules results in ambiguity for identifying oxy-tourmalines.

Table 5 shows that the empirical and calculated structural formulas of selected oxy-tourmaline species do not converge to same mineral name. In detail, sample PR1973 and TM84a can be only identified by the empirical structural formula. Sample PR85m is identified as oxy-schorl by the empirical formula and as oxy-dravite by the calculated formula. Sample drv18 is quite anomalous as both its empirical and its calculated formula lead to two new end-member formulas: $\text{Na}(\text{Mg}_2\text{Fe}^{3+})\text{Al}_6\text{Si}_6\text{O}_{18}(\text{BO}_3)_3(\text{OH})_3\text{O}$ and $\text{Na}(\text{Fe}_2^+\text{Fe}^{3+})\text{Al}_6\text{Si}_6\text{O}_{18}(\text{BO}_3)_3(\text{OH})_3\text{O}$, respectively. These formulas, however, appear to represent an unresolved issue in the classification scheme rather than the occurrence of new species.

The unsuccessful application of the procedure of Henry et al. (2013) for naming tourmaline species may be ascribed to inaccurately developed cation site distributions, concerning in particular: (1) the incorrect site preference of V^{3+} and Cr^{3+} for the Z site, which should be reversed as first ${}^Z\text{Cr}^{3+}$ and then ${}^Z\text{V}^{3+}$ (see above), and (2) the assumed qualitative Al site distribution, which incorrectly increases the actual amount of Al at the Z site. To improve this procedure, the site partitioning of important cations such as Al should be correctly modeled. Of particular relevance in this regard is the plot of ${}^Z\text{Al}$ vs. ${}^{[6]}\text{Al}$ ($= \text{Al}_{\text{tot}} - {}^Z\text{Al}$), obtained using cation-distribution data of 83 oxy-tourmalines accompanied by SREF, showing a strong positive nonlinear relation (Fig. 5). In detail, the plot displays the occurrence of an almost linear trend with ${}^Z\text{Al}/{}^{[6]}\text{Al}$ ratio very close to 1 for ${}^{[6]}\text{Al} < 4$ apfu, and a nonlinear trend for ${}^{[6]}\text{Al} > 4$ apfu. To make predic-

Skogby and the reviewers F.C. Hawthorne and A. Ertl for their useful suggestions that improved this work.

REFERENCES CITED

- Akizuki, M., Kuribayashi, T., Nagase, T., and Kitakaze, A. (2001) Triclinic liddicoatite and elbaite in growth sectors of tourmaline from Madagascar. *American Mineralogist*, 86, 364–369.
- Bačík, P., Cempírek, J., Uher, P., Novák, M., Ozdin, D., Filip, J., Škoda, R., Breiter, K., Klementová, M., and Duďa, R. (2013) Oxy-schorl, $\text{Na}(\text{Fe}^{2+}\text{Al})\text{Al}_6\text{Si}_6\text{O}_{18}(\text{BO}_3)_3(\text{OH})_2\text{O}$, a new mineral from Zlatá Idka, Slovak Republic and Příbyslavice, Czech Republic. *American Mineralogist*, 98, 485–492.
- Bačík, P., Ertl, A., Števko, M., Giester, G., and Sečkář, P. (2015) Acicular zoned tourmaline (magneso-foitite to foitite) from a quartz vein near Tisovec, Slovakia: the relationship between crystal chemistry and acicular habit. *Canadian Mineralogist*, 53, 221–234.
- Berryman, E.J., Wunder, B., Ertl, A., Koch-Müller, M., Rhede, D., Scheidl, K., Giester, G., and Heinrich, W. (2016) Influence of the X-site composition on tourmaline's crystal structure: Investigation of synthetic K-dravite, dravite, oxy-uvite, and magneso-foitite using SREF and Raman spectroscopy. *Physics and Chemistry of Minerals*, 43, 83–102.
- Bosi, F. (2008) Disordering of Fe^{2+} over octahedrally coordinated sites of tourmaline. *American Mineralogist*, 93, 1647–1653.
- (2010) Octahedrally coordinated vacancies in tourmaline: a theoretical approach. *Mineralogical Magazine*, 74, 1037–1044.
- (2011) Stereochemical constraints in tourmaline: from a short-range to a long-range structure. *Canadian Mineralogist*, 49, 17–27.
- (2013) Bond-valence constraints around the O1 site of tourmaline. *Mineralogical Magazine*, 77, 343–351.
- (2014) Mean bond length variation in crystal structures: a bond valence approach. *Acta Crystallographica*, B70, 697–704.
- Bosi, F., and Andreozzi, G.B. (2013) A critical comment on Ertl et al. (2012): “Limitations of Fe^{2+} and Mn^{2+} site occupancy in tourmaline: Evidence from Fe^{2+} - and Mn^{2+} -rich tourmaline. *American Mineralogist*, 98, 2183–2192.
- Bosi, F., and Lucchesi, S. (2007) Crystal chemical relationships in the tourmaline group: structural constraints on chemical variability. *American Mineralogist*, 92, 1054–1063.
- Bosi, F., and Skogby, H. (2013) Oxy-dravite, $\text{Na}(\text{Al}_2\text{Mg})(\text{Al}_3\text{Mg})(\text{Si}_6\text{O}_{18})(\text{BO}_3)_3(\text{OH})_2\text{O}$, a new mineral species of the tourmaline supergroup. *American Mineralogist*, 98, 1442–1448.
- Bosi, F., Balić-Zunić, T., and Surour, A.A. (2010) Crystal structure analysis of four tourmalines from the Cleopatra's Mines (Egypt) and Jabal Zalm (Saudi Arabia), and the role of Al in the tourmaline group. *American Mineralogist*, 95, 510–518.
- Bosi, F., Reznitskii, L., and Skogby, H. (2012) Oxy-chromium-dravite, $\text{NaCr}_3(\text{Cr}_4\text{Mg}_2)(\text{Si}_6\text{O}_{18})(\text{BO}_3)_3(\text{OH})_2\text{O}$, a new mineral species of the tourmaline supergroup. *American Mineralogist*, 97, 2024–2030.
- Bosi, F., Andreozzi, G.B., Skogby, H., Lussier, A.J., Abdu, Y., and Hawthorne, F.C. (2013a) Fluor-elbaite, $\text{Na}(\text{Li}_{1.5}\text{Al}_{1.5})\text{Al}_6(\text{Si}_6\text{O}_{18})(\text{BO}_3)_3(\text{OH})\text{F}$, a new mineral species of the tourmaline supergroup. *American Mineralogist*, 98, 297–303.
- Bosi, F., Reznitskii, L., and Sklyarov, E.V. (2013b) Oxy-vanadium-dravite, $\text{NaV}_3(\text{V}_4\text{Mg}_2)(\text{Si}_6\text{O}_{18})(\text{BO}_3)_3(\text{OH})_2\text{O}$: crystal structure and redefinition of the “vanadium-dravite” tourmaline. *American Mineralogist*, 98, 501–505.
- Bosi, F., Skogby, H., Hälenius, U., and Reznitskii, L. (2013c) Crystallographic and spectroscopic characterization of Fe-bearing chromo-alumino-povondrate and its relations with oxy-chromium-dravite and oxy-dravite. *American Mineralogist*, 98, 1557–1564.
- Bosi, F., Reznitskii, L., Skogby, H., and Hälenius, U. (2014a) Vanadio-oxy-chromium-dravite, $\text{NaV}_3(\text{Cr}_4\text{Mg}_2)(\text{Si}_6\text{O}_{18})(\text{BO}_3)_3(\text{OH})_2\text{O}$, a new mineral species of the tourmaline supergroup. *American Mineralogist*, 99, 1155–1162.
- Bosi, F., Skogby, H., Reznitskii, L., and Hälenius, U. (2014b) Vanadio-oxy-dravite, $\text{NaV}_3(\text{Al}_4\text{Mg}_2)(\text{Si}_6\text{O}_{18})(\text{BO}_3)_3(\text{OH})_2\text{O}$, a new mineral species of the tourmaline supergroup. *American Mineralogist*, 99, 218–224.
- Bosi, F., Andreozzi, G.B., Hälenius, U., and Skogby, H. (2015a) Experimental evidence for partial Fe^{2+} disorder at the Y and Z sites of tourmaline: a combined EMP, SREF, MS, IR and OAS study of schorl. *Mineralogical Magazine*, 79, 515–528.
- Bosi, F., Andreozzi, G.B., Agrosi, G., and Scandale, E. (2015b) Fluor-tsilaisite, $\text{NaMn}_3\text{Al}_6(\text{Si}_6\text{O}_{18})(\text{BO}_3)_3(\text{OH})\text{F}$, a new tourmaline from San Piero in Campo (Elba, Italy) and new data on tsilaisite tourmaline from the holotype specimen locality. *Mineralogical Magazine*, 79, 89–101.
- Bosi, F., Skogby, H., Lazor, P., and Reznitskii, L. (2015c) Atomic arrangements around the O3 site in Al- and Cr-rich oxy-tourmalines: a combined EMP, SREF, FTIR and Raman study. *Physics and Chemistry of Minerals*, 42, 441–453.
- Bosi, F., Skogby, H., and Hälenius, U. (2016a) Thermally induced cation redistribution in Fe-bearing oxy-dravite and potential geothermometric implications. *Contributions to Mineralogy and Petrology*, 171, 47.
- Bosi, F., Skogby, H., and Balić-Zunić, T. (2016b) Thermal stability of extended clusters in dravite: a combined EMP, SREF and FTIR study. *Physics and Chemistry of Minerals*, 43, 395–407.
- Bosi, F., Skogby, H., Ciriotti, M.E., Gadas, P., Novák, M., Cempírek, J., Všianský, D., and Filip, J. (2017a) Lucchesite, $\text{CaFe}^{2+}\text{Al}_4(\text{Si}_6\text{O}_{18})(\text{BO}_3)_3(\text{OH})_2\text{O}$, a new mineral species of the tourmaline supergroup. *Mineralogical Magazine*, 81, 1–14.
- Bosi, F., Reznitskii, L., Hälenius, U., and Skogby, H. (2017b) Crystal chemistry of Al-V-Cr oxy-tourmalines from Sludyanka complex, Lake Baikal, Russia. *European Journal of Mineralogy*, 29, 457–472.
- Bosi, F., Cámara, F., Ciriotti, M.E., Hälenius, U., Reznitskii, L., and Stagno, V. (2017c) Crystal-chemical relations and classification problems of tourmalines belonging to the oxy-schorl-oxy-dravite-bositite-povondrate series. *European Journal of Mineralogy*, 29, 445–455.
- Bosi, F., Skogby, H., and Hälenius, U. (2017d) Oxy-foitite, $\square(\text{Fe}^{2+}\text{Al})\text{Al}_4(\text{Si}_6\text{O}_{18})(\text{BO}_3)_3(\text{OH})_2\text{O}$, a new mineral species of the tourmaline supergroup. *European Journal of Mineralogy*, DOI: 10.1127/ejm/2017/0029-2631.
- Brown, I.D. (2016) *The chemical Bond in Inorganic Chemistry: The Bond Valence Model*, 2nd ed. Oxford University Press, U.K.
- Cámara, F., Ottolini, L., and Hawthorne, F.C. (2002) Crystal chemistry of three tourmalines by SREF, EMPA, and SIMS. *American Mineralogist*, 87, 1437–1442.
- Cempírek, J., Houzar, S., Novák, M., Groat, L.A., Selway, J.B., and Šrein, V. (2013) Crystal structure and compositional evolution of vanadium-rich oxy-dravite from graphite quartzite at Bítoványky, Czech Republic. *Journal of Geosciences*, 58, 149–162.
- Clark, C.M., Hawthorne, F.C., and Ottolini, L. (2011) Fluor-dravite, $\text{NaMg}_3\text{Al}_3\text{Si}_6\text{O}_{18}(\text{BO}_3)_3(\text{OH})_2\text{F}$, a new mineral species of the tourmaline group from the Crabtree emerald mine, Mitchell County, North Carolina: description and crystal structure. *Canadian Mineralogist*, 49, 57–62.
- Dutrow, B.L., and Henry, D.J. (2011) Tourmaline: A geologic DVD. *Elements*, 7, 301–306.
- Ertl, A., Hughes, J.M., Pertlik, F., Foit, F.F. Jr., Wright, S.E., Brandstätter, F., and Marler, B. (2002) Polyhedron distortions in tourmaline. *Canadian Mineralogist*, 40, 153–162.
- Ertl, A., Kolitsch, U., Prowatke, S., Dyar, M.D., and Henry, D.J. (2006) The F-analog of schorl from Grasstein, Trentino–South Tyrol, Italy: crystal structure and chemistry. *European Journal of Mineralogy*, 18, 583–588.
- Ertl, A., Hughes, J.M., Prowatke, S., Ludwig, T., Brandstätter, F., Körner, W., and Dyar, M.D. (2007) Tetrahedrally-coordinated boron in Li-bearing olenite from “mushroom” tourmaline from Momeik, Myanmar: structure and chemistry. *Canadian Mineralogist*, 45, 891–899.
- Ertl, A., Tillmanns, E., Ntaflos, T., Francis, C., Giester, G., Korner, W., Hughes, J.M., Lengauer, C., and Prem, M. (2008a) Tetrahedrally coordinated boron in Al-rich tourmaline and its relationship to the pressure-temperature conditions of formation. *European Journal of Mineralogy*, 20, 881–888.
- Ertl, A., Rossman, G.R., Hughes, J.M., Ma, C., and Brandstätter, F. (2008b) V^{3+} -bearing, Mg-rich, strongly disordered olenite from a graphite deposit near Amstall, Lower Austria: A structural, chemical and spectroscopic investigation. *Neues Jahrbuch für Mineralogie Abhandlungen*, 184, 243–253.
- Ertl, A., Kolitsch, U., Meyer, H.-P., Ludwig, T., Lengauer, C.L., Nasdala, L., and Tillmanns, E. (2009) Substitution mechanism in tourmalines of the “fluor-elbaite”-rossmanite series from Wolkenburg, Saxony, Germany. *Neues Jahrbuch für Mineralogie Abhandlungen*, 186, 51–61.
- Ertl, A., Rossman, G.R., Hughes, J.M., London, D., Wang, Y., O’Leary, J.A., Dyar, M.D., Prowatke, S., Ludwig, T., and Tillmanns, E. (2010a) Tourmaline of the elbaite-schorl series from the Himalaya Mine, Mesa Grande, California, U.S.A.: A detailed investigation. *American Mineralogist*, 95, 24–40.
- Ertl, A., Marschall, H.R., Giester, G., Henry, D.J., Schertl, H.-P., Ntaflos, T., Luvizotto, G.L., Nasdala, L., and Tillmanns, E. (2010b) Metamorphic ultra high-pressure tourmalines: Structure, chemistry, and correlations to *PT* conditions. *American Mineralogist*, 95, 1–10.
- Ertl, A., Mali, H., Schuster, R., Körner, W., Hughes, J.M., Brandstätter, F., and Tillmanns, E. (2010c) Li-bearing, disordered Mg-rich tourmalines from the pegmatite-marble contact from the Austroalpine basement units (Styria, Austria). *Mineralogy and Petrology*, 99, 89–104.
- Ertl, A., Schuster, R., Hughes, J.M., Ludwig, T., Meyer, H.-P., Finger, F., Dyar, M.D., Ruschel, K., Rossman, G.R., Klötzi, U., Brandstätter, F., Lengauer, C.L., and Tillmanns, E. (2012a) Li-bearing tourmalines in Variscan granitic pegmatites from the Moldanubian nappes, Lower Austria. *European Journal of Mineralogy*, 24, 695–715.
- Ertl, A., Giester, G., Ludwig, T., Meyer, H.-P., and Rossman, G.R. (2012b) Synthetic B-rich olenite: Correlations of single-crystal structural data. *American Mineralogist*, 97, 1591–1597.
- Ertl, A., Kolitsch, U., Dyar, M.D., Hughes, J.M., Rossman, G.R., Pieczka, A., Henry, D.J., Pezzotta, F., Prowatke, S., Lengauer, C.L., and others. (2012c) Limitations of Fe^{2+} and Mn^{2+} site occupancy in tourmaline: evidence from Fe^{2+} - and Mn^{2+} -rich tourmaline. *American Mineralogist*, 97, 1402–1416.
- Ertl, A., Giester, G., Schüssler, U., Brätz, H., Okrusch, M., Tillmanns, E., and Bank, H. (2013) Cu- and Mn-bearing tourmalines from Brazil and Mozambique: Crystal structures, chemistry and Correlations. *Mineralogy and Petrology*, 107, 265–279.
- Ertl, A., Vereshchagin, O.S., Giester, G., Tillmanns, E., Meyer, H.-P., Ludwig, T., Rozhdetsvenskaya, I.V., and Frank-Kamenetskaya, O.V. (2015) Structural and chemical investigation of a zoned synthetic Cu-rich tourmaline. *Canadian Mineralogist*, 53, 209–220.

- Ertl, A., Baksheev, I.A., Giester, G., Lengauer, C.L., Prokofiev, V.Y., and Zorina, L.D. (2016a) Bosiite, $\text{NaFe}_3(\text{Al}_4\text{Mg}_2)(\text{Si}_6\text{O}_{18})(\text{BO}_3)_2(\text{OH})_2\text{O}$, a new ferric member of the tourmaline supergroup from the Darasun gold deposit, Transbaikalia, Russia. *European Journal of Mineralogy*, 28, 581–591.
- Ertl, A., Kolitsch, U., Dyar, M.D., Meyer, H.-P., Henry, D.J., Rossman, G.R., Prem, M., Ludwig, T., Nasdala, L., Lengauer, C.L., Tillmanns, E., and Niedermayr, G. (2016b) Fluor-schorl, a new member of the tourmaline supergroup, and new data on schorl from the cotype localities. *European Journal of Mineralogy*, 28, 163–177.
- Filip, J., Bosi, F., Novák, M., Skogby, H., Tuček, J., Čuda, J., and Wildner, M. (2012) Redox processes of iron in the tourmaline structure: Example of the high-temperature treatment of Fe^{3+} -rich schorl. *Geochimica et Cosmochimica Acta*, 86, 239–256.
- Gatta, G.D., Danisi, R.M., Adamo, I., Meven, M., and Diella, V. (2012) A single-crystal neutron and X-ray diffraction study of elbaite. *Physics and Chemistry of Minerals*, 39, 577–588.
- Gatta, G.D., Bosi, F., McIntyre, G.J., and Skogby, H. (2014) First accurate location of two proton sites in tourmaline: A single-crystal neutron diffraction study of oxy-dravite. *Mineralogical Magazine*, 78, 681–692.
- Gibbs, G.V., Ross, N.L., Cox, D.F., and Rosso, K.M. (2014) Insights into the crystal chemistry of Earth materials rendered by electron density distributions: Pauling's rules revisited. *American Mineralogist*, 99, 1071–1084.
- Grew, E.S., Krivovichev, S.V., Hazen, R.M., and Hystad, G. (2016) Evolution of structural complexity in boron minerals. *Canadian Mineralogist*, 54, 125–143.
- Grew, E.S., Bosi, F., Gunter, M., Hälenius, U., Trumbull, R.B., and Yates, M.G. (2017) Fluor-elbaite, lepidolite and Ta-Nb oxides from a pegmatite of the 3000 MA Sinceni pluton, Swaziland: Evidence for lithium-cesium-tantalum (LCT) pegmatites in the Mesoarchean. *European Journal of Mineralogy*, DOI: 10.1127/ejm/2017/0029-2686.
- Hatert, F., and Burke, E.A.J. (2008) The IMA–CNMNC dominant-constituent rule revisited and extended. *Canadian Mineralogist*, 46, 717–728.
- Hawthorne, F.C. (1996) Structural mechanisms for light-element variations in tourmaline. *Canadian Mineralogist*, 34, 123–132.
- (2002) Bond-valence constraints on the chemical composition of tourmaline. *Canadian Mineralogist*, 40, 789–797.
- (Ed.) (2006) *Landmark Papers: Structure Topology*. The Mineralogical Society of Great Britain and Ireland, London.
- (2016) Short-range atomic arrangements in minerals. I: the minerals of the amphibole, tourmaline and pyroxene supergroups. *European Journal of Mineralogy*, 28, 513–536.
- Hawthorne, F.C., and Dirlam, D.M. (2011) Tourmaline the indicator mineral: from atomic arrangement to Viking navigation. *Elements*, 7, 307–312.
- Hawthorne, F.C., and Henry, D. (1999) Classification of the minerals of the tourmaline group. *European Journal of Mineralogy*, 11, 201–215.
- Hawthorne, F.C.H., Della Ventura, G., Oberti, R., Robert, J.-L., and Iezzi, G. (2005) Short-range order in minerals: amphiboles. *Canadian Mineralogist*, 43, 1895–1920.
- Henry, D.J., and Dutrow, B.L. (2011) The incorporation of fluorine in tourmaline: Internal crystallographic controls or external environmental influences? *Canadian Mineralogist*, 49, 41–56.
- Henry, D.J., Novák, M., Hawthorne, F.C., Ertl, A., Dutrow, B.L., Uher, P., and Pezzotta, F. (2011) Nomenclature of the tourmaline-supergroup minerals. *American Mineralogist*, 96, 895–913.
- Henry, D.J., Novák, M., Hawthorne, F.C., Ertl, A., Dutrow, B.L., Uher, P., and Pezzotta, F. (2013) Erratum. *American Mineralogist*, 98, 524.
- Hughes, J.M., Rakovan, J., Ertl, A., Rossman, G.R., Baksheev, I., and Bernhardt, H.-J. (2011) Dissymmetrization in tourmaline: the atomic arrangement of sectorally zoned triclinic Ni-bearing dravite. *Canadian Mineralogist*, 49, 29–40.
- Kihara, K., Hirata, H., Ida, A., Okudera, H., and Morishita, T. (2007) An X-ray single crystal study of asymmetric thermal vibrations and the positional disorder of atoms in elbaite. *Journal of Mineralogical and Petrological Sciences*, 102, 115–126.
- Krivovichev, S.V. (2013) Structural complexity of minerals: Information storage and processing in the mineral world. *Mineralogical Magazine*, 77, 275–326.
- Kutzbach, M., Wunder, B., Rhede, D., Koch-Müller, M., Ertl, A., Giester, G., Heinrich, W., and Franz, G. (2016) Tetrahedral boron in natural and synthetic high-pressure tourmaline: Evidence from Raman spectroscopy. *American Mineralogist*, 101, 93–104.
- Kutzbach, M., Wunder, B., Krstulovic, M., Ertl, A., Trumbull, R., Rocholl, A., and Giester, G. (2017) First high-pressure synthesis of rossmanitic tourmaline and evidence for the incorporation of Li at the X site. *Physics and Chemistry of Minerals*, 44, 353–363.
- London, D., Ertl, A., Hughes, J.M., Morgan, G.B. VI, Fritz, E.A., and Harms, B.S. (2006) Synthetic Ag-rich tourmaline: Structure and chemistry. *American Mineralogist*, 91, 680–684.
- Lussier, A.J., Aguiar, P.M., Michaelis, V.K., Kroeker, S., Herwig, S., Abdu, Y., and Hawthorne, F.C. (2008) Mushroom elbaite from the Kat Chay mine, Momeik, near Mogok, Myanmar: I. Crystal chemistry by SREF, EMPA, MAS NMR and Mössbauer spectroscopy. *Mineralogical Magazine*, 72, 747–761.
- Lussier, A.J., Hawthorne, F.C., Abdu, Y., Herwig, S., Michaelis, V.K., Aguiar, P.M., and Kroeker, S. (2011a) The crystal chemistry of “wheatstreak” tourmaline from Mogok, Myanmar. *Mineralogical Magazine*, 72, 999–1010.
- Lussier, A.J., Abdu, Y., Hawthorne, F.C., Michaelis, V.K., Aguiar, P.M., and Kroeker, S. (2011b) Oscillatory zoned liddicoatite from Anjanaboina, central Madagascar. I. Crystal chemistry and structure by SREF and ^{11}B and ^{27}Al MAS NMR spectroscopy. *Canadian Mineralogist*, 49, 63–88.
- Lussier, A., Ball, N.A., Hawthorne, F.C., Henry, D.J., Shimizu, R., Ogasawara, Y., and Ota, T. (2016) Maruyamaite, $\text{K}(\text{MgAl}_2)(\text{Al}_3\text{Mg})\text{Si}_6\text{O}_{18}(\text{BO}_3)_2(\text{OH})_2\text{O}$, a potassium-dominant tourmaline from the ultrahigh-pressure Kokchetav massif, northern Kazakhstan: description and crystal structure. *American Mineralogist*, 101, 355–361.
- Marler, B., Borowski, M., Wodara, U., and Schreyer, W. (2002) Synthetic tourmaline (olenite) with excess boron replacing silicon in the tetrahedral site: II. Structure analysis. *European Journal of Mineralogy*, 14, 763–771.
- Marschall, H.R., Korsakov, A.V., Luvizotto, G.L., Nasdala, L., and Ludwig, T. (2009) On the occurrence and boron isotopic composition of tourmaline in (ultra)high-pressure metamorphic rocks. *Journal of the Geological Society*, 166, 811–823.
- Nickel, E.H., and Grice, J.D. (1998) The IMA Commission on New Minerals and Mineral Names: procedures and guidelines on mineral nomenclature. *Canadian Mineralogist*, 36, 913–926.
- Nishio-Hamane, D., Minakawa, T., Yamaura, J., Oyama, T., Ohnishi, M., and Shimo-bayashi, N. (2014) Adachiite, a Si-poor member of the tourmaline supergroup from the Kiura mine, Oita Prefecture, Japan. *Journal of Mineralogical and Petrological Sciences*, 109, 74–78.
- Novák, M., Ertl, A., Povondra, P., Galiova, M.V., Rossman, G.R., Pristacz, H., Prem, M., Giester, G., Gadas, P., and Škoda, R. (2013) Darrellhenryite, $\text{Na}(\text{LiAl})\text{Al}_2(\text{BO}_3)_2\text{Si}_6\text{O}_{18}(\text{OH})_2\text{O}$, a new mineral from the tourmaline supergroup. *American Mineralogist*, 98, 1886–1892.
- Razmanova, Z.P., Kometova, V.A., Shipko, M.N., and Belov, N.B. (1983) Refinements in crystal structure and configuration of iron-bearing uvite. *Trudy AN SSSR, Mineralogicheskii Muзей im. A.E. Fersmana*, 31, 10–116 (in Russian).
- Reznitskii, L., Clark, C.M., Hawthorne, F.C., Grice, J.D., Skogby, H., Hälenius, U., and Bosi, F. (2014) Chromo-alumino-povondraite, $\text{NaCr}_3(\text{Al}_4\text{Mg}_2)(\text{Si}_6\text{O}_{18})(\text{BO}_3)_2(\text{OH})_2\text{O}$, a new mineral species of the tourmaline supergroup. *American Mineralogist*, 99, 1767–1773.
- Rozhdestvenskaya, I.V., Bronzova, Yu.M., Frank-Kamenetskaya, O.V., Zolotarev, A.A., Kuznetsova, L.G., and Bannova, I.I. (2008) Refinement of the crystal structure of calcium–lithium–aluminum tourmaline from the pegmatite vein in the Sangien Upland (Tuva Republic). *Crystallography Reports*, 53, 223–227.
- Rozhdestvenskaya, I.V., Setkovab, T.V., Vereshchagina, O.S., Shtukenberga, A.G., and Shapovalovb, Yu.B. (2012) Refinement of the crystal structures of synthetic nickel- and cobalt-bearing tourmalines. *Crystallography Reports*, 57, 57–63.
- Shannon, R.D. (1976) Revised effective ionic radii and systematic studies of interatomic distances in halides and chalcogenides. *Acta Crystallographica*, A32, 751–767.
- Shtukenberg, A., Rozhdestvenskaya, I., Frank-Kamenetskaya, O., Bronzova, J., Euler, H., Kirfel, A., Bannova, I., and Zolotarev, A. (2007) Symmetry and crystal structure of biaxial elbaite-liddicoatite tourmaline from the Transbaikalia region, Russia. *American Mineralogist*, 92, 675–686.
- Skogby, H., Bosi, F., and Lazor, P. (2012) Short-range order in tourmaline: a vibrational spectroscopic approach to elbaite. *Physics and Chemistry of Minerals*, 39, 811–816.
- van Hinsberg, V.J., Henry, D.J., and Marschall, H.R. (2011) Tourmaline: an ideal indicator of its host environment. *Canadian Mineralogist*, 49, 1–16.
- Vereshchagina, O.S., Rozhdestvenskaya, I.V., Frank-Kamenetskaya, O.V., Zolotarev, A.A., and Mashkovtsev, R.I. (2013) Crystal chemistry of Cu-bearing tourmalines. *American Mineralogist*, 98, 1610–1616.
- (2014) Ion substitutions and structural adjustment in Cr-bearing tourmalines. *European Journal of Mineralogy*, 26, 309–321.
- Vereshchagina, O.S., Frank-Kamenetskaya, O.V., and Rozhdestvenskaya, I.V. (2015) Crystal structure and stability of Ni-rich synthetic tourmaline. Distribution of divalent transition-metal cations over octahedral positions. *Mineralogical Magazine*, 79, 997–1006.
- Vereshchagina, O.S., Setkova, T.V., Rozhdestvenskaya, I.V., Frank-Kamenetskaya, O.V., Deyneko, D.V., and Pokholok, K.V. (2016) Synthesis and crystal structure of Ga-rich, Fe-bearing tourmaline. *European Journal of Mineralogy*, 28, 593–599.
- Watenphul, A., Burgdorf, M., Schlüter, J., Horn, I., Malcherek, T., and Mihailova, B. (2016) Exploring the potential of Raman spectroscopy for crystallographic analyses of complex hydrous silicates: II. Tourmalines. *American Mineralogist*, 101, 970–985.